Published in final edited form as:
Bioconjug Chem. 2012 February 15; 23(2): 158–163. doi:10.1021/bc2004507.

Fluorescent Peptide-PNA Chimeras for Imaging Monoamine Oxidase A mRNA in Neuronal Cells

Dalip Sethi[1], **Chang-Po Chen**[1], **Rui-Yan Jing**[1], **Mathew L. Thakur**[2,3], and **Eric Wickstrom**[1,3,*]

[1]Department of Biochemistry & Molecular Biology, Thomas Jefferson University, Philadelphia, PA 19107

[2]Department of Radiology, Thomas Jefferson University, Philadelphia, PA 19107

[3]Kimmel Cancer Center, Thomas Jefferson University, Philadelphia, PA 19107

Abstract

Monoamine oxidases (MAO) catalyze the oxidative deamination of many biogenic amines and are integral proteins found in the mitochondrial outer membrane. Changes in MAO-A levels are associated with depression, trait aggression and addiction. Here we report the synthesis, characterization and *in-vitro* evaluation of novel fluorescent peptide-peptide nucleic acid (PNA) chimeras for *MAOA* mRNA imaging in live neuronal cells. The probes were designed to include *MAOA*-specific PNA dodecamers, separated by an N-terminal spacer to a μ-opioid receptor targeting peptide (DAMGO), with a spacer and a fluorophore on the C-terminus. The probe was successfully delivered into human SH-SY5Y neuroblastoma cells through μ-opioid receptor-mediated endocytosis. The K_d by flow cytometry was 11.6 ± 0.8 nM. Uptake studies by fluorescence microscopy showed ~5-fold higher signal in human SH-SY5Y neuroblastoma cells than in negative control CHO-K1 cells that lack μ-opioid receptors. Moreover, a peptide-mismatch control sequence showed no significant uptake in SH-SY5Y cells. Such mRNA imaging agents with near infrared fluorophores might enable real time imaging and quantitation of neuronal mRNAs in live animal models.

Keywords

DAMGO; fluorescence; hybridization; μ-opioid receptor; monoamine oxidase A; peptide nucleic acid

Monoamine oxidases (MAO) catalyze the oxidative deamination of many biogenic amines. MAO are expressed in various neuronal and non-neuronal cells in the central nervous system (CNS) and peripheral organs[1]. In the CNS, MAO carries out metabolic inactivation of released monoamine transmitters, but also creates cytotoxic free radicals throughout aging and neurodegenerative diseases. MAO exists in two isoforms, MAO-A and MAO-B, which differ by their substrate specificity and more for inhibitor selectivity. MAO-A preferentially deaminates serotonin, dopamine, and norepinephrine in catecholaminergic neurons in the human brain, in particular, adrenergic and noradrenergic neurons. On the other hand, MAO-B preferentially degrades exogenous bioamines ingested in the diet such as phenylethylamine and benzylamine. The catalytic activity of MAO-A, located in the

*Corresponding author. Phone: 215.955.4578, Fax: 215.955.4580. eric@tesla.jci.tju.edu.

SUPPORTING INFORMATION AVAILABLE

Additional data on synthesis and experimental results with *MAOA* probes are available free of charge via the Internet at http://pubs.acs.org/.

mitochondria of presynaptic terminals in monoamine-releasing neurons, have a critical role in regulating the release and degradation of monoamines throughout the brain[2, 3].

Differential expression of the *MAOA* gene, called by some the "warrior gene", has been linked to numerous CNS disorders, particularly aggression[4–6], antisocial behavior, attention deficit hyperactivity disorder[7, 8], anxiety[9], anorexia nervosa[10, 11], bipolar disorder[12–14], drug abuse[15, 16] and Alzheimer's disease[17]. Elevated MAO-A levels in affect modulating regions are believed to exert an important monoamine-lowering process during key depressive episodes of major depressive disorder. In postpartum depression, MAO-A levels and affinity increase sharply due to a decline (100- to 1000-fold) in estrogen levels, which creates a high risk for depressive episodes[18].

On the other hand, genetic deletion of *MAOA* produces aggressive phenotypes across species. Studies have found links between *MAOA* gene products and violent behavior. Lower MAO-A activity in cortical and sub-cortical brain regions results in higher self-reported trait aggression[19]. MAO-A also plays a critical role in alcohol[20, 21] and cocaine addiction[22]. A recent study showed up-regulated MAO-A expression in alcoholic individuals, using whole genome sequencing of mRNA transcripts (RNA-Seq)[21]. In another study, *MAOA*-L (low repeat allele) carrier males with cocaine use disorders (CUD) revealed greater grey matter volume (GMV) reduction in the brain as compared to their healthy counterparts[22]. Over the last two decades, positron emission tomography (PET) has been used extensively for measuring MAO-A enzyme activity in different tissues[3]. ^{11}C-clorgyline is one of the example of compounds used for such studies[23]. However, no such method is available for non-invasive measurement of *MAOA* mRNA expression.

The objective of the present study was to develop an *MAOA* mRNA imaging agent composed of a complementary peptide nucleic acid (PNA) labeled with a fluorescent dye for imaging, and attached to a peptide moiety for receptor-mediated intracellular delivery. PNA, an oligonucleotide analog where the sugar-phophodiester backbone is replaced with a peptide-like aminoethylglycine backbone, has great potential for biomedical applications[24, 25]. Owing to their achiral, uncharged, flexible backbone, PNAs hybridize with mRNA more strongly than normal RNA or DNA with mRNA. They are resistant to enzymatic degradation and are stable over a wide range of pH. However, due to its uncharged nature, naked PNA is poorly taken up by mammalian cells[26].

As a result, incorporation of a receptor-targeting peptide is an efficient way to deliver PNA imaging agents into targeted cells[25]. To specifically target our probes to neuronal cells, we extended a modified DAMGO μ-opioid targeting peptide, Tyr-D-Ala-Gly-NMePhe-Ser, from the N-terminus of PNA. DAMGO is an enkephalin analog that binds tightly to μ-opioid receptors on neuronal cells and induces internalization[27]. The phenolic hydroxyl (−OH) group of the N-terminal Tyr residue with a free cationic α-amino ($-NH_3^+$) group, similar to the tyramine moiety of morphine, and an aromatic amino acid separated by one or two residues, are the core requirements for the binding of opioid peptides[28]. The replacement of the glycinol moiety with L-serine maintains receptor affinity (K_i value 0.56 ± 0.006 nM for DAMGO with glycinol, 0.68 ± 0.02 nM for DAMGO with L-serine)[29].

Here we report the synthesis, characterization and *in-vitro* evaluation of peptide-PNA-fluorophore chimeras for *MAOA* mRNA imaging. A receptor-specific agent, Tyr-D-Ala-Gly-N-MePhe-Ser-AEEA-CAT GGT GCT CAC-AEEA-Cys-AlexaFluor488 (WT4879) (Figure 1), and a peptide mismatch control, Ala-D-Ala-Gly-N-MePhe-Ser-AEEA-CAT GGT GCT CAC-AEEA-Cys-AlexaFluor488 (WT4786) were synthesized by Fmoc-based solid phase coupling (Supporting Information, Scheme S1). The chimeras were purified using reverse phase-high performance liquid chromatography (RP-HPLC) using C_{18}

columns (Figure 2) and characterized by mass spectrometry. AlexaFluor488-maleimide (Invitrogen, Carlsbad CA) was coupled to the C-terminal cysteine thiols in aqueous buffer under standard conditions. The human neuroblastoma cell line SH-SY5Y (ATCC), which expresses both μ-opioid receptor and *MAOA* mRNA[30, 31], was used for *in-vitro* studies of agent uptake. SH-SY5Y cells were maintained in a 1:1 (v/v) DMEM:F12 medium supplemented with 10% fetal bovine serum (FBS). Chinese hamster ovarian cells, CHO-K1 (ATCC), were used as a negative control. CHO-K1 cells were maintained in Ham's F12 medium containing 10% FBS. Cells were incubated at 37°C under 5% CO_2 in a humidified chamber.

In order to determine the K_d for WT4879, a competition binding assay was performed. In brief, 4×10^4 SH-SY5Y cells/tube were incubated with a ramp of concentrations (0, 4, 8 16, 32, 64 and 128 nM) of WT4879 (with and without 20× free DAMGO peptide, Set I and II) for 1 h at 4°C in the dark. After incubation, cells were washed twice with cold 1× calcium-magnesium-free phosphate buffered saline, CMF-PBS-5, containing 5% FBS, to remove the unbound probe. Subsequently, cells were fixed with CMF-PBS-5 + 1% paraformaldehyde for 10 min at 25°C in the dark, washed twice with CMF-PBS-5, resuspended in 300 μL of CMF-PBS-5, and analyzed on a FACS Calibur flow cytometer (BD Biosciences, San Jose, CA). In each case, the fluorescence intensities of 5,000 vital cells were acquired. Vital cells were gated based on sideward and forward scatter. To calculate specific uptake, both non-specific uptake with 20x free DAMGO and background were subtracted from total uptake. The K_d was found to be 11.6 ± 0.8 nM.

To evaluate the specificity of uptake, a ramp of concentrations (0.1, 0.2, 0.35 and 0.5 μM) of WT4879 (receptor-specific agent) and WT4786 (peptide mismatch agent) were prepared in 1:1 (v/v) DMEM:F12 medium. 2×10^5 SH-SY5Y cells/well were cultured in 6-well plates to ~70 % confluence and the cells were incubated with imaging agent solutions for 6 h at 37°C under 5% CO_2 in a humidified incubator. After incubation, cells were washed with cold CMF-PBS-5 (3 mL) and detached using 0.05% trypsin. The cells were washed and fixed as described above and finally re-suspended in 300 μL of CMF-PBS-5 for flow cytometry. 25,000 vital cells were screened for each sample. A ratio of specific over non-specific uptake was calculated and plotted against concentration (μM) (Figure 3). The results revealed that specificity of uptake follows an inverse relationship to the concentration of the probe. At 0.1 μM, WT4879 probe showed ~5-fold higher uptake than WT4786, indicating high uptake specificity. A similar experiment was performed using the CHO-K1 negative control cell line in Ham's F12 medium. The specificity ratio for WT4879 was found to be 1 ± 0.3 at all the concentrations, implying no specific uptake in cells lacking the μ-opioid receptor.

The results of the above experiments were used to evaluate the time course of agent uptake. Briefly, 6.5×10^4 SH-SY5Y cells were seeded in each well of a poly-D-lysine coated 4-well micro-slide (BD Biosciences) one day before the experiment. Cells were incubated with 0.1 μM WT4879 for increasing times (0, 0.25, 0.5, 1, 2, 4, 8 and 12 h) at 37°C in a humidified chamber with 5% CO_2. After the incubation, cells were washed twice with CMF-PBS-5 and fixed using 4% paraformaldehyde in CMF-PBS-5 for 15 min. Prolong Gold Antifade (Invitrogen) with DAPI, was used as mounting media for micro-slides. The slides were visualized using a LSM 510 Meta confocal microscope (Zeiss, New York NY) using the 488 nm line of an argon ion laser with a BP 505–550 nm band pass filter. DAPI was visualized using a 405-nm diode laser. Following image acquisition, images were quantified with ImageJ software (http://rsbweb.nih.gov/ij). No significant uptake was observed at 0.25 and 0.5 h (data not shown). WT4879 was taken up strongly after 1 h and found to be uniformly distributed in the cytoplasm (Figure 4). The uptake intensity increased with time up to 4 h, leveling off thereafter.

In order to study the specificity for receptor-targeted delivery, a comparative uptake study was performed using CHO-K1 (1.5×10^4 cells/well) and SH-SY5Y (6.5×10^4 cells/well) by the same protocol, as described above. Cells were incubated for 4 h at 37°C with 0.1 μM WT4879 and WT4786 in respective growth media. Three fields were quantitated on each slide. The results revealed that negative control CHO-K1 cells took up ~21% as much receptor-specific WT4879 agent as did SH-SY5Y cells (Figure 5A,C). In SH-SY5Y cells, the peptide mismatch WT4786 agent showed ~20% uptake relative to the specific WT4879 (Figure 5B,C), consistent with the receptor-specific uptake observed by flow cytometry. In a structural control experiment, an agent with a fluorophore on the N-terminus, and DAMGO on the C-terminus, showed similar low uptake by SH-SY5Y cells (data not shown), consistent with the requirement for a free N-terminal cationic amine on DAMGO[28].

Following the specificity study, a live cell study was performed to evaluate the uptake mechanism of WT4879 in SH-SY5Y cells. Briefly, 2×10^5 cells/dish were seeded in 35 mm dishes (μ-dishes, ibidi GmbH, Germany) and transfected with CellLight BacMam reagent (Invitrogen), according to the manufacturer's protocol (Invitrogen), to label early endosomes with RFP-labeled Rab5 protein. After the expression of RFP-labeled Rab5 protein, cells were incubated for 1 h at 37°C with 0.1 μM WT4879 in phenol red-free growth medium. The dishes were washed with phenol red-free medium (3 × 2 mL) and visualized using a heated stage on the LSM 510 Meta confocal microscope. The cells showed co-localization of WT4879 with Rab5 in early endosomes (Figure 6ABC). The same section of each dish was scanned after additional 1 h incubation at 37°C. The endosomes disappeared and WT4879 was found to be uniformly distributed in the cytoplasm (Figure 6DEF). The control cells expressed RFP-labeled Rab5 but did not showed any green fluorescence. The intensities of RFP for labeled Rab5 and AlexaFluor 488 for WT4879 were measured along the x-axis using Amira 5 software, which showed >95% overlap (Supporting Information, Figure S1). These results imply receptor-specific uptake of WT4879 into early endosomes, followed by cytosolic dispersal of cargo.

The toxicity of WT4879 on SH-SY5Y cells was measured with a Vybrant MTT Cell Proliferation Assay Kit (Invitrogen). Briefly, cells were seeded in 96-well microtiter plates (2×10^4 cells/well) and cultivated overnight in phenol red-free DMEM:F12 medium (Invitrogen). Subsequently, SH-SY5Y cells were incubated with three concentrations (0.1, 0.5 and 1 μM) of WT4879 for 12 h at 37°C. Cells were then incubated with MTT dye at a concentration of 1 mg/mL for 4 h. The formazan product was solubilized with Me_2SO (50 μL). Cell viability was determined by measuring the absorbance of each sample at 540 nm using a microplate reader. The cells exposed to increasing concentrations of WT4879 survived just as well as control cells (Supporting Information, Figure S2). No cellular toxicity was observed at any concentration tested, suggesting the biocompatibility of the synthesized probes.

In conclusion, a new *MAOA* mRNA imaging agent, coupled to a receptor-targeting peptide for specific intracellular delivery, was designed and synthesized. Initial *in-vitro* studies demonstrated that WT4879 was specifically delivered to SH-SY5Y cells, which express μ-opioid receptors and *MAOA* mRNA, with high efficiency. The receptor-specific probe (WT4879) showed ~5 times higher uptake than the non-specific probe (WT4786), in SH-SY5Y cells, using flow cytometry and confocal microscopy. The control cell-line (CHO-K1) showed minimal non-specific uptake of WT4879. Moreover, an MTT assay of WT4879 revealed high compatibility with SH-SY5Y cells. Such mRNA imaging agents, with near infrared fluorophores, might enable real time imaging and quantitation of neuronal mRNAs in live animal models.

Supplementary Material

Refer to Web version on PubMed Central for supplementary material.

Acknowledgments

We thank Dr. Andrew Quong for mass spectrometry. This work was supported by NIH grant DA027746 to E.W. M.L.T. and E.W. hold shares in GeneSeen LLC, which might ultimately benefit from the results of this investigation, but did not support the work.

Abbreviations

AEEA	aminoethoxyethoxyacetyl
DAPI	4′,6-diamidino-2-phenylindole
MAO	monoamine oxidase
MTT	3-(4,5-dimethylthiazol-2-yl)-2,5-diphenyltetrazolium bromide
PBS	phosphate buffered saline
PNA	peptide nucleic acid

References

1. Rendu F, Peoc'h K, Berlin I, Thomas D, Launay JM. Smoking Related Diseases: The Central Role of Monoamine Oxidase. Int J Environ Res Public Health. 2011; 8:136–147. [PubMed: 21318020]
2. Bolasco A, Carradori S, Fioravanti R. Focusing on new monoamine oxidase inhibitors. Expert Opin Ther Pat. 2010; 20:909–39. [PubMed: 20553094]
3. Fowler JS, Logan J, Volkow ND, Wang GJ. Translational neuroimaging: positron emission tomography studies of monoamine oxidase. Mol Imaging Biol. 2005; 7:377–87. [PubMed: 16265597]
4. Brunner HG, Nelen M, Breakefield XO, Ropers HH, van Oost BA. Abnormal behavior associated with a point mutation in the structural gene for monoamine oxidase A. Science. 1993; 262:578–80. [PubMed: 8211186]
5. Manuck SB, Flory JD, Ferrell RE, Mann JJ, Muldoon MF. A regulatory polymorphism of the monoamine oxidase-A gene may be associated with variability in aggression, impulsivity, and central nervous system serotonergic responsivity. Psychiatry Res. 2000; 95:9–23. [PubMed: 10904119]
6. Newman TK, Syagailo YV, Barr CS, Wendland JR, Champoux M, Graessle M, Suomi SJ, Higley JD, Lesch KP. Monoamine oxidase A gene promoter variation and rearing experience influences aggressive behavior in rhesus monkeys. Biol Psychiatry. 2005; 57:167–72. [PubMed: 15652876]
7. Jiang S, Xin R, Lin S, Qian Y, Tang G, Wang D, Wu X. Linkage studies between attention-deficit hyperactivity disorder and the monoamine oxidase genes. Am J Med Genet. 2001; 105:783–8. [PubMed: 11803531]
8. Lawson DC, Turic D, Langley K, Pay HM, Govan CF, Norton N, Hamshere ML, Owen MJ, O'Donovan MC, Thapar A. Association analysis of monoamine oxidase A and attention deficit hyperactivity disorder. Am J Med Genet B Neuropsychiatr Genet. 2003; 116B:84–9. [PubMed: 12497620]
9. Tadic A, Rujescu D, Szegedi A, Giegling I, Singer P, Moller HJ, Dahmen N. Association of a MAOA gene variant with generalized anxiety disorder, but not with panic disorder or major depression. Am J Med Genet B Neuropsychiatr Genet. 2003; 117B:1–6. [PubMed: 12555227]
10. Urwin RE, Bennetts BH, Wilcken B, Lampropoulos B, Beumont PJ, Russell JD, Tanner SL, Nunn KP. Gene-gene interaction between the monoamine oxidase A gene and solute carrier family 6 (neurotransmitter transporter, noradrenalin) member 2 gene in anorexia nervosa (restrictive subtype). Eur J Hum Genet. 2003; 11:945–50. [PubMed: 14508509]

11. Urwin RE, Nunn KP. Epistatic interaction between the monoamine oxidase A and serotonin transporter genes in anorexia nervosa. Eur J Hum Genet. 2005; 13:370–5. [PubMed: 15523490]
12. Gutierrez B, Arias B, Gasto C, Catalan R, Papiol S, Pintor L, Fananas L. Association analysis between a functional polymorphism in the monoamine oxidase A gene promoter and severe mood disorders. Psychiatr Genet. 2004; 14:203–8. [PubMed: 15564894]
13. Preisig M, Bellivier F, Fenton BT, Baud P, Berney A, Courtet P, Hardy P, Golaz J, Leboyer M, Mallet J, Matthey ML, Mouthon D, Neidhart E, Nosten-Bertrand M, Stadelmann-Dubuis E, Guimon J, Ferrero F, Buresi C, Malafosse A. Association between bipolar disorder and monoamine oxidase A gene polymorphisms: results of a multicenter study. Am J Psychiatry. 2000; 157:948–55. [PubMed: 10831475]
14. Rubinsztein DC, Leggo J, Goodburn S, Walsh C, Jain S, Paykel ES. Genetic association between monoamine oxidase A microsatellite and RFLP alleles and bipolar affective disorder: analysis and meta-analysis. Hum Mol Genet. 1996; 5:779–82. [PubMed: 8776592]
15. Huang YY, Cate SP, Battistuzzi C, Oquendo MA, Brent D, Mann JJ. An association between a functional polymorphism in the monoamine oxidase a gene promoter, impulsive traits and early abuse experiences. Neuropsychopharmacology. 2004; 29:1498–505. [PubMed: 15150530]
16. Vanyukov MM, Maher BS, Devlin B, Tarter RE, Kirillova GP, Yu LM, Ferrell RE. Haplotypes of the monoamine oxidase genes and the risk for substance use disorders. Am J Med Genet B Neuropsychiatr Genet. 2004; 125B:120–5. [PubMed: 14755456]
17. Takehashi M, Tanaka S, Masliah E, Ueda K. Association of monoamine oxidase A gene polymorphism with Alzheimer's disease and Lewy body variant. Neurosci Lett. 2002; 327:79–82. [PubMed: 12098640]
18. Sacher J, Wilson AA, Houle S, Rusjan P, Hassan S, Bloomfield PM, Stewart DE, Meyer JH. Elevated brain monoamine oxidase A binding in the early postpartum period. Arch Gen Psychiatry. 2010; 67:468–74. [PubMed: 20439828]
19. Alia-Klein N, Goldstein RZ, Kriplani A, Logan J, Tomasi D, Williams B, Telang F, Shumay E, Biegon A, Craig IW, Henn F, Wang GJ, Volkow ND, Fowler JS. Brain monoamine oxidase A activity predicts trait aggression. J Neurosci. 2008; 28:5099–104. [PubMed: 18463263]
20. Mokrovic G, Matosic A, Hranilovic D, Stefulj J, Novokmet M, Oreskovic D, Balija M, Marusic S, Cicin-Sain L. Alcohol dependence and polymorphisms of serotonin-related genes: association studies. Coll Antropol. 2008; 32(Suppl 1):127–31. [PubMed: 18405071]
21. Zhou Z, Yuan Q, Mash DC, Goldman D. Substance-specific and shared transcription and epigenetic changes in the human hippocampus chronically exposed to cocaine and alcohol. Proc Natl Acad Sci U S A. 2011; 108:6626–31. [PubMed: 21464311]
22. Alia-Klein N, Parvaz MA, Woicik PA, Konova AB, Maloney T, Shumay E, Wang R, Telang F, Biegon A, Wang GJ, Fowler JS, Tomasi D, Volkow ND, Goldstein RZ. Gene × disease interaction on orbitofrontal gray matter in cocaine addiction. Arch Gen Psychiatry. 2011; 68:283–94. [PubMed: 21383264]
23. Fowler JS, MacGregor RR, Wolf AP, Arnett CD, Dewey SL, Schlyer D, Christman D, Logan J, Smith M, Sachs H, et al. Mapping human brain monoamine oxidase A and B with 11C-labeled suicide inactivators and PET. Science. 1987; 235:481–5. [PubMed: 3099392]
24. Nielsen PE. Peptide nucleic acids (PNA) in chemical biology and drug discovery. Chem Biodivers. 2010; 7:786–804. [PubMed: 20397216]
25. Ray A, Norden B. Peptide nucleic acid (PNA): its medical and biotechnical applications and promise for the future. FASEB J. 2000; 14:1041–60. [PubMed: 10834926]
26. Gray GD, Basu S, Wickstrom E. Transformed and immortalized cellular uptake of oligodeoxynucleoside phosphorothioates, 3′-alkylamino oligodeoxynucleotides, 2′-O-methyl oligoribonucleotides, oligodeoxynucleoside methylphosphonates, and peptide nucleic acids. Biochemical Pharmacology. 1997; 53:1465–1476. [PubMed: 9260874]
27. Wang Y, Van Bockstaele EJ, Liu-Chen LY. In vivo trafficking of endogenous opioid receptors. Life Sci. 2008; 83:693–9. [PubMed: 18930741]
28. Borics A, Toth G. Structural comparison of mu-opioid receptor selective peptides confirmed four parameters of bioactivity. J Mol Graph Model. 2010; 28:495–505. [PubMed: 20036591]

29. Lowery JJ, Yeomans L, Keyari CM, Davis P, Porreca F, Knapp BI, Bidlack JM, Bilsky EJ, Polt R. Glycosylation improves the central effects of DAMGO. Chem Biol Drug Des. 2007; 69:41–7. [PubMed: 17313456]

30. Muller T, Przuntek H, Rieks M, Mackowiak A. Selegiline reduces cisplatin-induced neuronal death in neuroblastoma cells. Neurol Res. 2008; 30:417–9. [PubMed: 18237459]

31. Toll L. Mu-opioid receptor binding in intact SH-SY5Y neuroblastoma cells. Eur J Pharmacol. 1990; 176:213–7. [PubMed: 1968847]

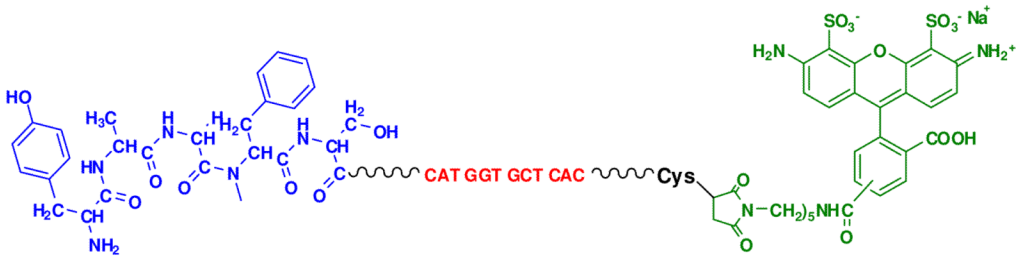

Figure 1.

ChemDraw representation of WT4879. Targeting peptide (blue) is linked to PNA (red) at N-terminus and to AlexaFluor488 (green) at C-terminus via thiol-maleimide linkage.

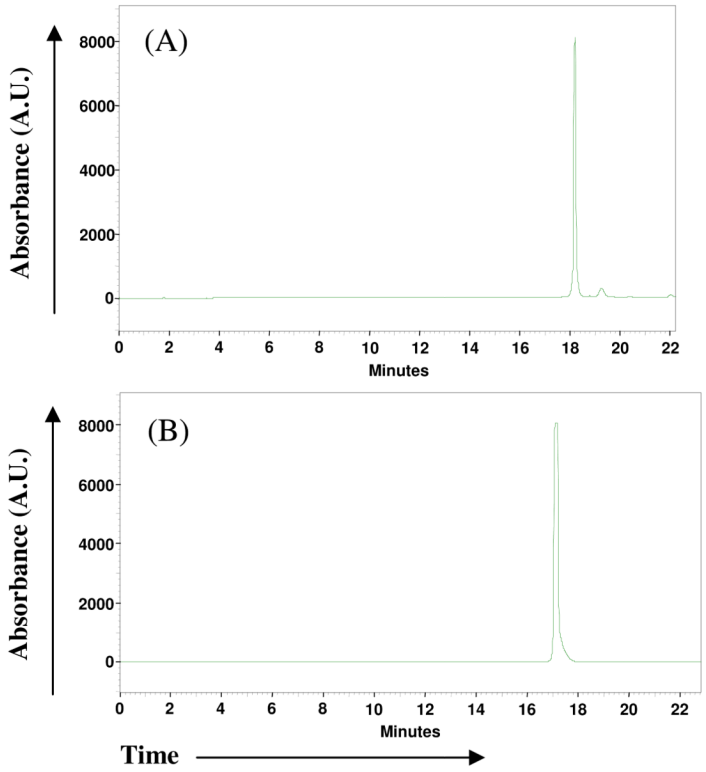

Figure 2.

HPLC profiles of (A) Tyr-D-Ala-Gly-N-MePhe-Ser-AEEA-CAT GGT GCT CAC-AEEA-Cys-AlexaFluor488, WT4879 [DAMGO-MAOA-AlexaFluor488, m/z 4878.78 (calculated), 4879.20 (observed)]; and (B) Ala-D-Ala-Gly-N-MePhe-Ser-AEEA-CAT GGT GCT CAC-AEEA-Cys-AlexaFluor488, WT4786 [peptide-mismatch-MAOA-AlexaFluor488, m/z 4786.78 (calculated), 4786.08 (observed)] on a 10 × 250 mm Alltima C_{18} column, eluted at 2.5 ml/min with a 30-min gradient from 5% to 60% CH_3CN in aqueous 0.1% CF_3CO_2H, at 50°C, monitored at 488 nm.

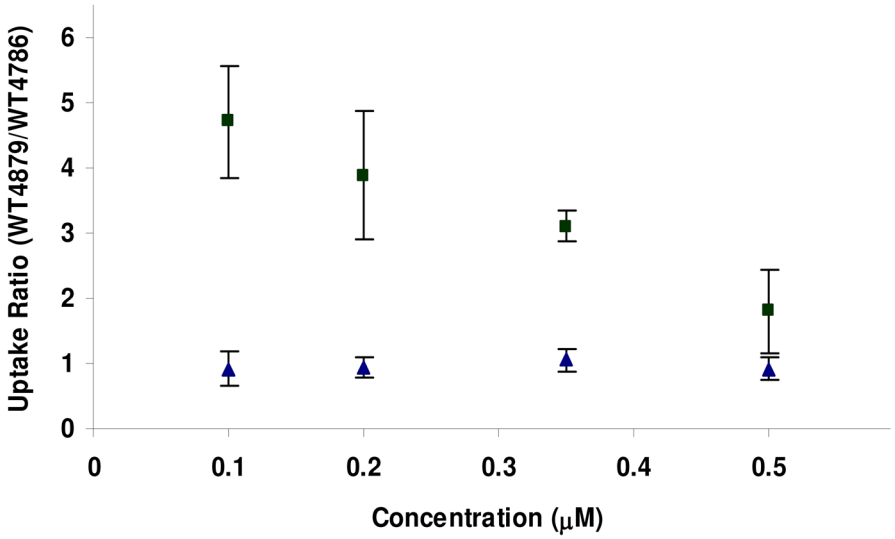

Figure 3.

Specificity of uptake in SH-SY5Y (■) and CHO-K1 (▲) cells of WT4879 (μ-opioid receptor-specific agent) vs. WT4786 (peptide mismatch agent) over a ramp of concentrations measured by flow cytometry. Ratios of specific to non-specific uptake, after background correction, were calculated and plotted against concentration (μM), averaged over three replicate experiments.

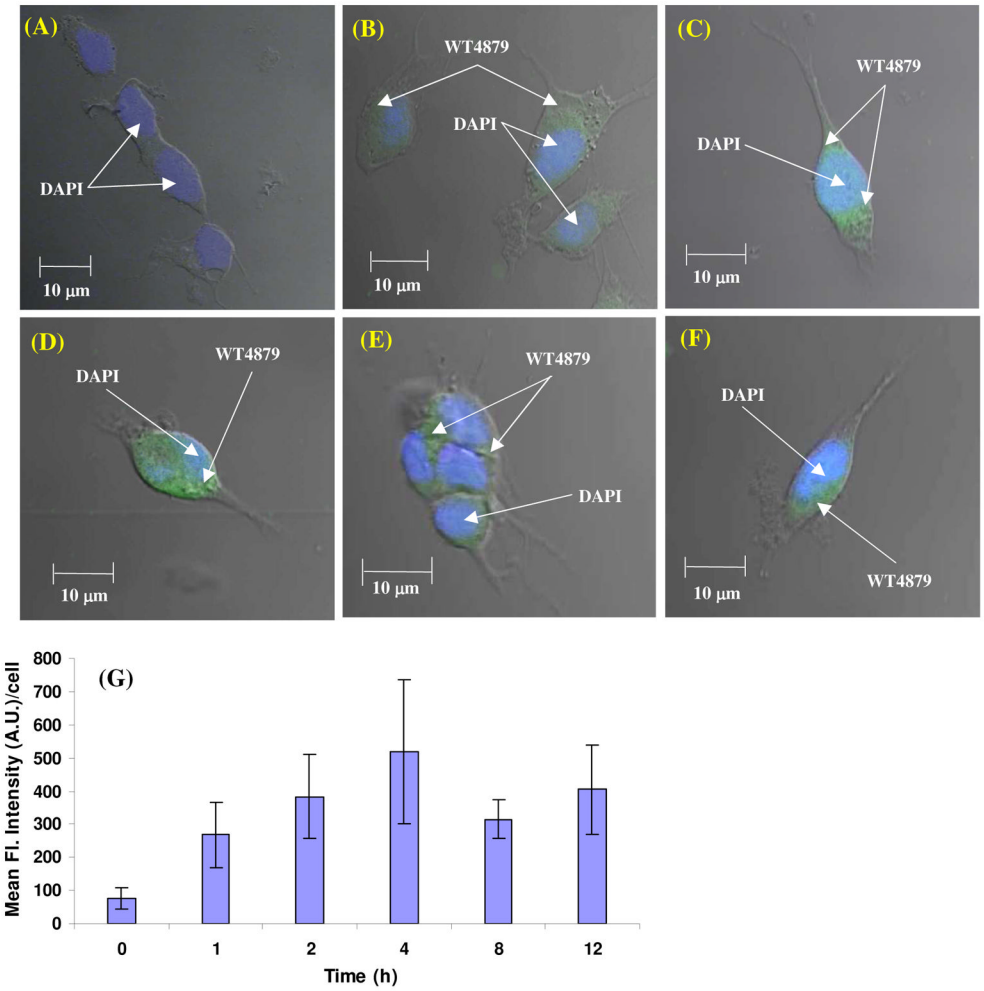

Figure 4.

Confocal fluorescent images of WT4879 uptake in SH-SH5Y cells (A) Control, (B) After 1 h, (C) 2 h, (D) 4 h, (E) 8 h, (F) 12 h, and (G) histogram showing mean fluorescence intensity (arbitrary units, A.U.) per cell measured at different times, averaged over three regions of interest.

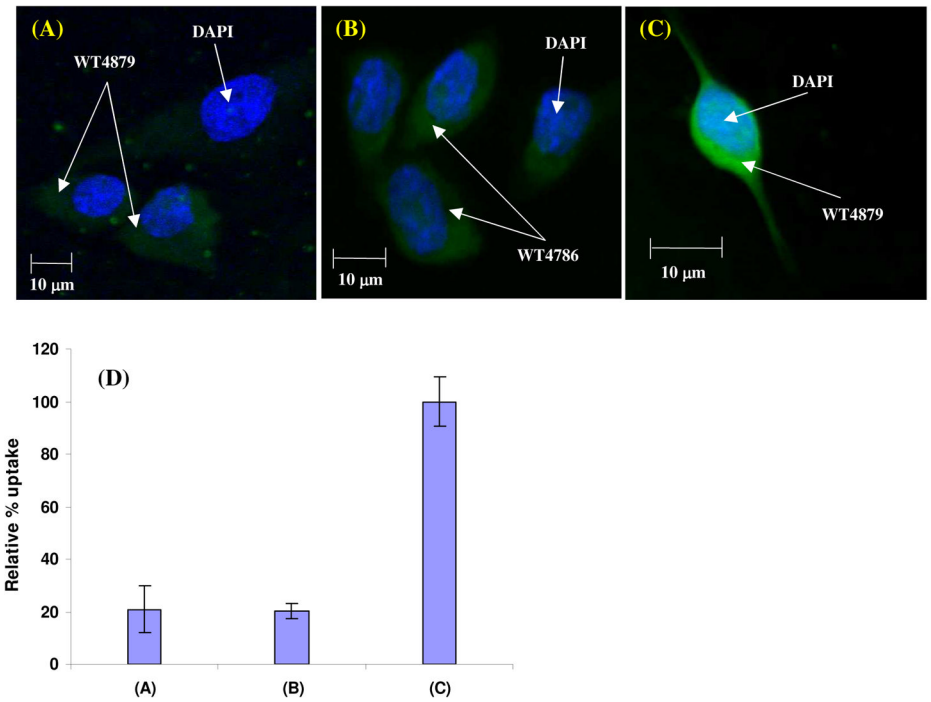

Figure 5.

Confocal fluorescent images of (A) WT4879 uptake in CHO-K1 cells, (B) WT4786 uptake in SH-SH5Y cells, (C) WT4879 uptake in SH-SY5Y cells after 4 h of incubation at 37°C with 0.1 μM agent in respective growth media and (D) histogram showing the relative percent of uptake for 3 fields on each slide.

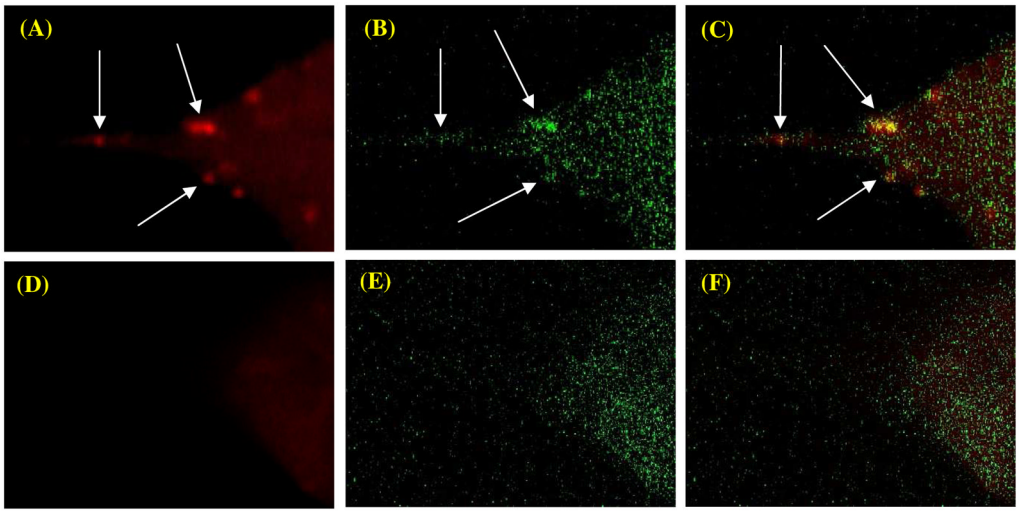

Figure 6.

Confocal fluorescent images of live SH-SY5Y cells showing the (A) localization of RFP-labeled Rab5, (B) WT4879 in endosomes, (C) co-localization of RFP labeled Rab5 and WT4879, (D) RFP-labeled Rab5, (E) WT4879 distribution in cells after an additional 1 h incubation at 37°C and (F) merged image of (D) & (E).